THE THIN LENS MODEL IN THE SECOND ORDER AND SOME EFFECTS DUE TO LINEAR COUPLING*

V. GARCZYNSKI

Alternating Gradient Synchrotron, Brookhaven National Laboratory, Upton, NY 11973, USA

The Thin Lens Model is extended to higher order in the skew-quadrupole strengths and is applied to a discussion of various effects due to linear coupling. Beta-function distortions, tune splitting, and tune shift are calculated up to the second order in the skew-quadrupole errors. The single-turn transfer matrix, to the second order, is given. The Thick Ellipse Effect as a possible tool for the coupling diagnosis is elaborated in some detail, to the first order. The well known Brown and Servranckx treatment of the emittance change in a transfer line is extended to include a ring case as well.

1 INTRODUCTION

The Thin Lens Model (TLM) is useful in describing and in correcting effects of skew-quadrupole errors in large circular accelerators.[1-5] Usually the linear, in the skew-quad strengths approximation works well.[6-8] However, in case of rings made of superconducting magnets, which are prone to larger errors, the higher-order terms, it seems, should be also included. In RHIC, for example, a residual tune-splitting, quadratic in skew-quadrupole errors, was found in computer simulations.[9]

In the paper we describe an extension of the TLM to higher orders, using the so called "projection" approach.[6-7] The second-order terms are displayed in detail, while the path to higher-order terms is clearly outlined. A different approach to the TLM in higher-orders was proposed by Ruggiero,[10] who also considered the stability and the tune-splitting problems. Because of this we shall just mention these two topics briefly , using our notation, and proceed with a discussion of the other linear coupling effects.[11-12] The emittance growth due to linear coupling[13] and the Thick Ellipse Effect[14] will be treated to first order only.

---

2   THE TLM IN THE SECOND-ORDER

Consider a ring of circumference C containing N thin skew quadrupoles of strengths $q_1, \ldots, q_N$ and locations

$$0 < s_1 < \cdots < s_N < C. \tag{2.1}$$

Assume that a transfer matrix of an ideal ring (that is, a ring without the skew quadrupoles) is known, and is of the (decoupled) form

$$T_0(s'', s') = \left[\begin{array}{c|c} T_{0x}(s'', s') & 0 \\ \hline 0 & T_{0y}(s'', s') \end{array} \right]. \tag{2.2}$$

Passing to the circular representation (normalized coordinates), $\overset{\circ}{z} = \mathcal{B}z$, we get

$$T_0(s'', s') = \mathcal{B}^{-1}(s'') \overset{\circ}{T}_0 (s'', s') \mathcal{B}(s'), \tag{2.3}$$

where

$$\mathcal{B} = \left[\begin{array}{c|c} \mathcal{B}_x & 0 \\ \hline 0 & \mathcal{B}_y \end{array} \right], \tag{2.4}$$

$$\mathcal{B}_{x,y} = \left[\begin{array}{cc} \beta^{-1/2} & 0 \\ \alpha\beta^{-1/2} & \beta^{1/2} \end{array} \right]_{x,y}, \mathcal{B}_{x,y}^{-1} = \left[\begin{array}{cc} \beta^{1/2} & 0 \\ -\alpha\beta^{-1/2} & \beta^{-1/2} \end{array} \right]_{x,y}, \tag{2.5}$$

and

$$\overset{\circ}{T}_0 (s'', s') = \left[\begin{array}{c|c} R[\psi_x(s'', s')] & 0 \\ \hline 0 & R[\psi_y(s'', s')] \end{array} \right], \tag{2.6}$$

$R(\psi_{x,y})$ are rotations

$$R(\psi) = \left[\begin{array}{c|c} \cos(\psi) & \sin(\psi) \\ \hline -\sin(\psi) & \cos(\psi) \end{array} \right], \tag{2.7}$$

and $\psi_{x,y}$ are the phase advances

$$\psi_{x,y}(s'', s') = \int_{s'}^{s''} \frac{ds}{\beta_{x,y}(s)}. \tag{2.8}$$

The lattice functions $\alpha_{x,y}, \beta_{x,y}$ are C-periodic in their argument.

The single-turn transfer matrix

$$\overset{\circ}{T} = \overset{\circ}{T}(C, 0), \tag{2.9}$$

where we took $s = 0$ as a reference point, can be written as follows:

$$\overset{\circ}{T} \equiv \begin{bmatrix} \overset{\circ}{M} & \overset{\circ}{n} \\ \overset{\circ}{m} & \overset{\circ}{N} \end{bmatrix} = \mathcal{B}T\mathcal{B}^{-1} = \begin{bmatrix} \mathcal{B}_x M \mathcal{B}_x^{-1} & \mathcal{B}_x n \mathcal{B}_y^{-1} \\ \mathcal{B}_y m \mathcal{B}_x^{-1} & \mathcal{B}_y N \mathcal{B}_y^{-1} \end{bmatrix} = \sum_{k=0}^{N} \overset{\circ}{T}^{(k)}, \tag{2.10}$$

where $\overset{\circ}{T}^{(k)}$ is a k-th order, homogeneous polynomial in the skew-quadrupole strengths. For instance, the 2×2 submatrices $\overset{\circ}{M}, \overset{\circ}{n}, \overset{\circ}{m}$ and $\overset{\circ}{N}$ can be written through the first-order $d^{(1)}$ and second-order $d^{(2)}$ driving terms as follows:

$$\overset{\circ}{M}_{11} = \cos\mu_x - d_{SC}^{(2)}\cos\mu_x + d_{CC}^{(2)}\sin\mu_x + 0(q^4), \tag{2.11}$$

$$\overset{\circ}{M}_{12} = \sin\mu_x - d_{SS}^{(2)}\cos\mu_x + d_{CS}^{(2)}\sin\mu_x + 0(q^4), \tag{2.12}$$

$$\overset{\circ}{M}_{21} = -\sin\mu_x + d_{CC}^{(2)}\cos\mu_x + d_{SC}^{(2)}\sin\mu_x + 0(q^4), \tag{2.13}$$

$$\overset{\circ}{M}_{22} = \cos\mu_x + d_{CS}^{(2)}\cos\mu_x + d_{SS}^{(2)}\sin\mu_x + 0(q^4); \tag{2.14}$$

and

$$\overset{\circ}{N}_{kl} = (\overset{\circ}{M}_{kl})^{\vee}, \qquad k, l = 1, 2; \tag{2.15}$$

and

$$\overset{\circ}{n}_{11} = -d_{SC}^{(1)}\cos\mu_x + d_{CC}^{(1)}\sin\mu_x + 0(q^3), \tag{2.16}$$

$$\overset{\circ}{n}_{12} = -d_{SS}^{(1)}\cos\mu_x + d_{CS}^{(1)}\sin\mu_x + 0(q^3), \tag{2.17}$$

$$\overset{\circ}{n}_{21} = d_{CC}^{(1)}\cos\mu_x + d_{SC}^{(1)}\sin\mu_x + 0(q^3), \tag{2.18}$$

$$\overset{\circ}{n}_{22} = d_{CS}^{(1)}\cos\mu_x + d_{SS}^{(1)}\sin\mu_x + 0(q^3); \tag{2.19}$$

and

$$\overset{\circ}{m}_{kl} = (\overset{\circ}{n}_{kl})^{\vee}, \qquad k, l = 1, 2. \tag{2.20}$$

Here the notation is:

$$\begin{bmatrix} d_{SS}^{(1)} \\ d_{SC}^{(1)} \\ d_{CS}^{(1)} \\ d_{CC}^{(1)} \end{bmatrix} = \sum_{r=1}^{N} q_r \begin{bmatrix} \sin\mu_x^r \sin\mu_y^r \\ \sin\mu_x^r \cos\mu_y^r \\ \cos\mu_x^r \sin\mu_y^r \\ \cos\mu_x^r \cos\mu_y^r \end{bmatrix}, \tag{2.21}$$

and for the second-order driving terms,

$$
\begin{bmatrix} d^{(2)}_{SS} \\ d^{(2)}_{SC} \\ d^{(2)}_{CS} \\ d^{(2)}_{CC} \end{bmatrix} = \sum_{1 \le r < s \le N} q_r q_s \sin(\mu^s_y - \mu^r_y) \begin{bmatrix} \sin \mu^s_x \sin \mu^r_x \\ \sin \mu^s_x \cos \mu^r_x \\ \cos \mu^s_x \sin \mu^r_x \\ \cos \mu^s_x \cos \mu^r_x \end{bmatrix}, \tag{2.22}
$$

where μ^r_x, μ^r_y are phase advances

$$
\mu^r_x = \int_0^{s_r} \frac{ds}{\beta_x} \equiv \psi_x(s_r, 0), \tag{2.23}
$$

and similarly for the μ^r_y.

The thin skew-quadrupole strengths are

$$
q_k = (\beta_x \beta_y)^{1/2} f_k^{-1} \big|_{s_k}, \quad k = 1, \ldots, N. \tag{2.24}
$$

The "$\vee$" operation replaces x with y and x' with y'.

For example, for the first-order driving terms we get

$$
\begin{aligned}
(d^{(1)}_{CC})^\vee &= d^{(1)}_{CC}, \\
(d^{(1)}_{SS})^\vee &= d^{(1)}_{SS}, \\
(d^{(1)}_{CS})^\vee &= d^{(1)}_{SC}, \\
(d^{(1)}_{SC})^\vee &= d^{(1)}_{CS}.
\end{aligned} \tag{2.25}
$$

Similar but less symmetric results follow for the second-order driving terms. In particular, the relations hold:

$$
\det n \equiv |n| = d^{(1)}_{SS} d^{(1)}_{CC} - d^{(1)}_{SC} d^{(1)}_{CS} = d^{(2)}_{SC} - d^{(2)}_{CS} = \overset{\vee}{d}{}^{(2)}_{SC} - \overset{\vee}{d}{}^{(2)}_{CS}. \tag{2.26}
$$

The outline of the derivation of these results is given in Appendix A. In the next chapters we shall consider some applications of the TLM.

Assuming that the q's are normally distributed random variables, i.e., that

$$
\langle q_r \rangle = 0, \tag{2.27}
$$

and

$$
\langle q_r q_s \rangle = G_0^2 / N \, \delta_{rs}, \quad r, s = 1, \ldots, N, \tag{2.28}
$$

and also assuming that, for both x and y directions,

$$\langle \sin \mu^r \rangle = \langle \cos \mu^r \rangle = 0, \tag{2.29}$$

and

$$\langle \sin^2 \mu^r \rangle = \langle \cos^2 \mu^r \rangle = 1/2, \tag{2.30}$$

while the averages of mixed products assumed to vanish, we get for the averages of the driving terms

$$\langle d^{(1)} \rangle = 0, \tag{2.31}$$

$$\langle d^{(2)} \rangle = 0, \tag{2.32}$$

$$\langle d^{(1)^2} \rangle = G_0^2/4, \tag{2.33}$$

and similarly for the $\check{d}$-driving terms.

The averages of the squares of the second-order driving terms are small, and the averages of products of the different first-order driving terms vanish. Thus, for example, we get the results

$$\langle |n| \rangle = 0 + \ldots , \tag{2.34}$$

$$\langle |n|^2 \rangle = \frac{1}{8} G_0^4 + \ldots . \tag{2.35}$$

The parameters G_0 takes on these values for the Relativistic Heavy-Ion Collider and the Superconducting Super Collider:

$$G_0 \simeq 0.25, \quad \text{for RHIC}, \tag{2.36}$$

and

$$G_0 \simeq 0.5 - 1.0, \text{ for SSC}. \tag{2.37}$$

3 THE STABILITY PROBLEM

If T is the single-turn symplectic transfer matrix of the form

$$T = \begin{bmatrix} M & n \\ m & N \end{bmatrix}, \tag{3.1}$$

having eigenvalues λ_1, λ_1^{-1}, λ_2, λ_2^{-1} then the sums

$$\Lambda_k = \lambda_k + \lambda_k^{-1}, \quad k = 1, 2 \tag{3.2}$$

are given by the well-known formulae[1]

$$\Lambda_{1,2} = 2 \cos \mu_{1,2} = \frac{1}{2} Tr(M + N) \pm \left(\left[\frac{1}{2} Tr(M - N) \right]^2 + |\overline{m} + n| \right)^{1/2}, \tag{3.3}$$

where $\mu_{1,2}$ are, called the "new" tunes. All the elements appearing there can be easily expressed through the driving terms (see Appendix B).

The stability conditions

$$1^o \quad \Lambda_k - \text{ real}, \tag{3.4}$$

$$2^o \quad |\Lambda_k| \le 2, \quad k = 1, 2, \tag{3.5}$$

can be satisfied most easily near the resonance, $\mu_x = \mu_y$, because the determinant $|\overline{m} + n|$ is positive in this case.

4   THE TUNE SPLITTING

Let the new tunes $\mu_{1,2}$ differ slightly from the old ones:

$$\mu_1 = \mu_x + 2\pi \Delta\nu_1 , \quad \mu_2 = \mu_y + 2\pi \Delta\nu_2, \quad (\mu_x > \mu_y). \tag{4.1}$$

From Equation (3.3), one then gets

$$\Delta\nu_1 = \frac{1}{2\pi} \cot \mu_x - \frac{1}{8\pi \sin \mu_x} Tr(M + N)$$

$$- \frac{1}{4\pi \sin \mu_x} \left(\left[\frac{1}{2} Tr(M - N) \right]^2 + |\overline{m} + n| \right)^{1/2} + \cdots , \tag{4.2}$$

and

$$\Delta\nu_2 = \frac{1}{2\pi} \cot \mu_y - \frac{1}{8\pi \sin \mu_y} Tr(M + N)$$

$$+ \frac{1}{4\pi \sin \mu_y} \left(\left[\frac{1}{2} Tr(M - N) \right]^2 + |\overline{m} + n| \right)^{1/2} + \cdots . \tag{4.3}$$

The leading terms, on the resonance $\mu_x = \mu_y$, are

$$\Delta\nu_1 = -\,\text{sgn}(\sin\mu_x)\frac{1}{4\pi}\left[\left(d_{SC}^{(1)} + d_{CS}^{(1)}\right)^2 + \left(d_{CC}^{(1)} + d_{SS}^{(1)}\right)^2\right]^{1/2} + \cdots, \qquad (4.4)$$

and

$$\Delta\nu_2 = -\Delta\nu_1 . \qquad (4.5)$$

Here we used Equation (B.13) (see Appendix B) for the determinant $|\overline{m} + n|$. This can be viewed as a generalized "Golden Rule"[4] since the above combination of the first-order driving terms is of the first-order in the q's:

$$\left[\left(d_{SC}^{(1)} + d_{CS}^{(1)}\right)^2 + \left(d_{CC}^{(1)} + d_{SS}^{(1)}\right)^2\right]^{1/2} = \left|\sum_{k=1}^{N} q_k e^{i(\mu_x^k - \mu_y^k)}\right|. \qquad (4.6)$$

The higher-order terms in the expansions of $\frac{1}{2}Tr(M \pm N)$ contribute to the "residual" tune-splitting, which persists after all the first-order driving terms are corrected:

$$\Delta\nu_{1_{\text{resid}}} = -\frac{1}{8\pi}\left(d_{CC}^{(2)} + d_{SS}^{(2)} + \overset{\vee(2)}{d_{CC}} + \overset{\vee(2)}{d_{SS}}\right) +$$

$$- \text{sgn}(\sin\mu_x)\frac{1}{8\pi}\left|d_{CC}^{(2)} + d_{SS}^{(2)} - \overset{\vee(2)}{d_{CC}} - \overset{\vee(2)}{d_{SS}}\right| + \cdots, \qquad (4.7)$$

and

$$\Delta\nu_{2_{\text{resid}}} = -\frac{1}{8\pi}\left(d_{CC}^{(2)} + d_{SS}^{(2)} + \overset{\vee(2)}{d_{CC}} + \overset{\vee(2)}{d_{SS}}\right)$$

$$+ \text{sgn}(\sin\mu_x)\frac{1}{8\pi}\left|d_{CC}^{(2)} + d_{SS}^{(2)} - \overset{\vee(2)}{d_{CC}} - \overset{\vee(2)}{d_{SS}}\right| \cdots. \qquad (4.8)$$

In-order to correct the tune-splitting up to the second order, one requires that: the local correction scheme at $s = 0$ satisfy

$$d_{SS}^{(1)} = d_{SC}^{(1)} = d_{CS}^{(1)} = d_{CC}^{(1)} = 0, \qquad (4.9)$$

and

$$d_{CC}^{(2)} + d_{SS}^{(2)} = 0, \qquad (4.10)$$

and

$$\overset{\vee(2)}{d_{CC}} + \overset{\vee(2)}{d_{SS}} = 0. \qquad (4.11)$$

Clearly, the tune splitting vanishes under these conditions. The last two conditions can be expressed through the q's as follows:

$$d_{CC}^{(2)} + d_{SS}^{(2)} - \overset{\vee(2)}{d_{CC}} - \overset{\vee(2)}{d_{SS}} = \sum_{r<s} q_r q_s \sin(\delta_r - \delta_s) = 0, \tag{4.12}$$

and

$$d_{CC}^{(2)} + d_{SS}^{(2)} + \overset{\vee(2)}{d_{CC}} + \overset{\vee(2)}{d_{SS}} = -\sum_{r<s} q_r q_s \sin(\sigma_r - \sigma_s) = 0, \tag{4.13}$$

where.

$$\delta_r = \mu_x^r - \mu_y^r, \tag{4.14}$$

and

$$\sigma_r = \mu_x^r + \mu_y^r. \tag{4.15}$$

5   THE TUNE SHIFT

Owing to the basic formulae of Equations (2.11)–(2.15), one finds for the traces of the submatrices M and N the expressions

$$\begin{aligned} \frac{1}{2} TrM &= \left(1 - \frac{1}{2}|n|\right) \cos \mu_x + \frac{1}{2}\left(d_{CC}^{(2)} + d_{SS}^{(2)}\right) \sin \mu_x + \cdots \\ &= \cos(\mu_x + \Delta\mu_x), \end{aligned} \tag{5.1}$$

and

$$\begin{aligned} \frac{1}{2} TrN &= \left(1 - \frac{1}{2}|n|\right) \cos \mu_y + \frac{1}{2}\left(\overset{\vee(2)}{d_{CC}} + \overset{\vee(2)}{d_{SS}}\right) \sin \mu_y + \cdots \\ &= \cos(\mu_y + \Delta\mu_y). \end{aligned} \tag{5.2}$$

Hence for a small tune shift $\Delta\mu_x$, $\Delta\mu_y$ we obtain

$$\Delta\mu_x = \frac{1}{2}|n| \cot \mu_x - \frac{1}{2}\left(d_{CC}^{(2)} + d_{SS}^{(2)}\right) + \cdots, \tag{5.3}$$

and

$$\Delta\mu_y = \frac{1}{2}|n| \cot \mu_y - \frac{1}{2}\left(\overset{\vee(2)}{d_{CC}} + \overset{\vee(2)}{d_{SS}}\right) + \cdots. \tag{5.4}$$

Notice that the tune shift vanishes at the point where the tune-splitting correction was done.

6 THE BETA FUNCTION DISTORTIONS

The new beta functions are given by (cf. Equations (B.9) and (B.11) in Appendix B)

$$\beta_1 = (\sin\mu_1)^{-1}A_{12} = \beta_x + \Delta\beta_x, \tag{6.1}$$

and

$$\beta_2 = (\sin\mu_2)^{-1}B_{12} = \beta_y + \Delta\beta_y, \tag{6.2}$$

where $\Delta\beta_{x,y}$ are the beta-function distortions. Taking into account Equations (B.8) and (B.10), we get the results

$$
\begin{aligned}
\frac{\Delta\beta_x}{\beta_x} &= -1 + (\beta_x\sin\mu_x)^{-1}M_{12} - 2\pi\Delta\nu_1\cot\mu_x \\
&\quad + [\beta_x\sin\mu_x(t+\delta)]^{-1}[(\overline{m}+n)m]_{12} + \cdots,
\end{aligned}
\tag{6.3}
$$

and

$$
\begin{aligned}
\frac{\Delta\beta_y}{\beta_y} &= -1 + (\beta_y\sin\mu_y)^{-1}N_{12} - 2\pi\Delta\nu_2\cot\mu_y \\
&\quad - [\beta_y\sin\mu_y(t+\delta)]^{-1}[(m+\overline{n})n]_{12} + \cdots.
\end{aligned}
\tag{6.4}
$$

The leading terms, on the resonance $\mu_x = \mu_y$, are

$$\frac{\Delta\beta_x}{\beta_x} = \frac{1}{2}\,\text{sgn}(\sin\mu_x)\cot\mu_x\left|\sum_{k=1}^{N}q_k e^{i(\mu_x^k-\mu_y^k)}\right| + \cdots, \tag{6.5}$$

and

$$\frac{\Delta\beta_y}{\beta_y} = -\frac{\Delta\beta_x}{\beta_x}. \tag{6.6}$$

The residual beta-function distortions remain after the tune-splitting is locally corrected:

$$\frac{\Delta\beta_x}{\beta_x}\bigg|_{\Delta\nu=0} = d_{CC}^{(2)} - d_{SS}^{(2)}\cot\mu_x + \cdots, \tag{6.7}$$

and

$$\frac{\Delta\beta_y}{\beta_y}\bigg|_{\Delta\nu=0} = -\overset{\vee(2)}{d_{CS}} - \overset{\vee(2)}{d_{SS}}\cot\mu_y + \cdots. \tag{6.8}$$

From Equations (6.5) and (6.6) we get the following rms estimates of the leading-order beta-function distortions (on the resonance $\mu_x = \mu_y$):

$$\left(\frac{\Delta\beta_x}{\beta_x}\right)_{\text{rms}} = \left(\frac{\Delta\beta_y}{\beta_y}\right)_{\text{rms}} = \frac{1}{2}G_0|\cot\mu_x|. \qquad (6.9)$$

Substituting the relevant RHIC parameters,

$$\mu_x = 2\pi \times 28.827, \quad \mu_y = 2\pi \times 28.823$$

$$G_0 = 0.25, \qquad\qquad\qquad (6.10)$$

we get

$$\left(\frac{\Delta\beta}{\beta}\right)_{\text{rms}} = 0.14, \qquad \text{(RHIC)}. \qquad (6.11)$$

7   THE THICK ELLIPSE EFFECT

Coupling between the transverse x and y degrees of freedom causes phase plots (x, x') or (y, y') that are thick ellipses (the Thick Ellipse Effect). This effect is seen in computer simulations of the x-y coupling existing in RHIC: a smear of the familiar Courant-Snyder ellipses (or, rather, circles in suitably normalized coordinates) is produced in both the (x, x') and the (y, y')-planes. The smear presented in Fig. 1 corresponds to plotting of the (x, x'), and (y, y') components of a finite number of points (1000) in a discrete set of points:

$$T(z_0), T(T(z_0)), \ldots, \underbrace{T(\cdots T(T(z_0))\cdots)}_{1000}, \qquad (7.1)$$

where T is a single-turn map that includes all the x-y coupling, not just the linear one. Thus the example is not a perfect one for comparison with our results presented below, which do not take into account the coupling produced by sextupoles and higher-order multipoles. Also, we do not stick to just one initial vector z_0 as in the example. Presumably more of the phase space would be covered if a variety of initial vectors were employed and a larger number of turns considered.

In this paper we examine the linearly coupled motion produced by thin skew-quadrupoles distributed around a ring and determine their contribution to the Thick Ellipse Effect. We reveal the main driving terms responsible for the spread of the invariant curves. We also show that the spread is removed at the point where the tune splitting correction is made.

In-order to be able to accommodate any trajectory, corresponding to any choice of initial conditions and number of turns, we are looking for the total areas in the physical subspaces, i.e., the (x, x'), (y, y') and (x, y) subspaces, that are available for
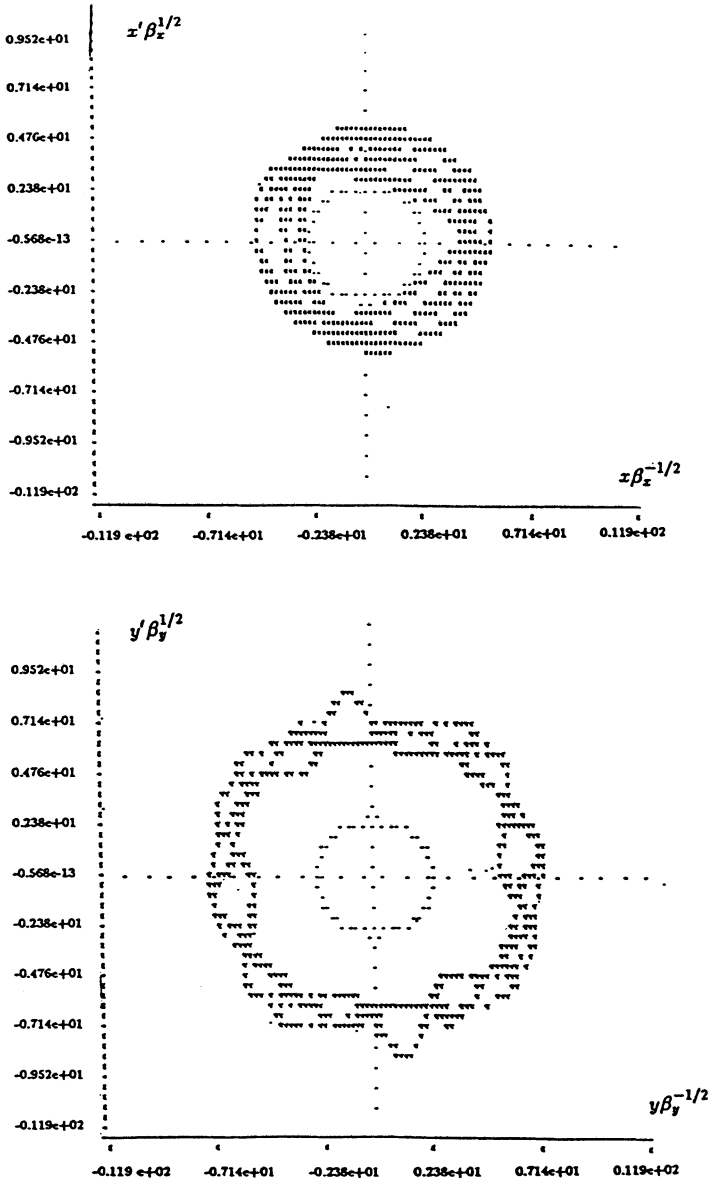
FIGURE 1: The Thick Ellipse Effect in computer simulations of the x-y coupling in RHIC (courtesy of G. Fritz Dell).

the motion. They are given by projections of the invariant 4-ellipsoid that replace the familiar Courant-Snyder curves when the linear coupling is present. We study this rather novel object in some detail first.

As usual, $\partial\mathcal{E}_4$ denotes a two-dimensional surface of the solid four-dimensional $\mathcal{E}_4$; similarly for the lower-dimensional geometric objects appearing in the sequel. We will estimate the effect to the first-order in the skew-quadrupole strengths since it is, usually, sufficient. We hope that the detailed treatment of the effect will result in a tool for diagnosis of the linear coupling.

We consider the betatron motion under presence of the linear coupling produced by skew-quadrupole fields. The Hamiltonian of the system is quadratic with the C-periodic coefficients

$$H = \frac{1}{2}p_x^2 + \frac{1}{2}p_y^2 + \frac{1}{2}(\rho^{-2} - k)x^2 + \frac{1}{2}ky^2 - Nxy. \tag{7.2}$$

Corresponding coupled Hamilton's equations are linear, and their solution can be written in the form

$$z(s) = T(s, s_0)z(s_0). \tag{7.3}$$

It is well known[2] that there exists a real symplectic matrix R such that when passing to new variables $w = R^{-1}z$

$$w = \begin{bmatrix} u \\ u' \\ v \\ v' \end{bmatrix} = \begin{pmatrix} U \\ V \end{pmatrix}, \tag{7.4}$$

the motions decouple, i.e.,

$$w(s) = U(s, s_0)w(s_0),$$

and, cf. Equations (B.1)–(B.11),

$$U = R^{-1}TR = \begin{pmatrix} A & 0 \\ 0 & B \end{pmatrix}. \tag{7.5}$$

The submatrices A, B are real 2×2 symplectic matrices describing uncoupled normal motions. In particular their powers are given by

$$A^n = e^{n\mu_1 \mathbf{J}_1} = \mathbf{1}_2 \cos(n\mu_1) + \mathbf{J}_1 \sin(n\mu_1), \tag{7.6}$$

$$B^n = e^{n\mu_2 \mathbf{J}_2} = \mathbf{1}_2 \cos(n\mu_2) + \mathbf{J}_2 \sin(n\mu_2), \tag{7.7}$$

where the matrices $\mathbf{J}_k$ are C-periodic and symplectic:

$$\mathbf{J}_k = \begin{pmatrix} \alpha_k & \beta_k \\ -\gamma_k & -\alpha_k \end{pmatrix}, \tag{7.8}$$

$$|\mathbf{J}_k| = \beta_k\gamma_k - \alpha_k^2 = 1, \tag{7.9}$$

and

$$\mathbf{J}_k^2 = -\mathbf{1}_k \quad , \quad k = 1, 2. \tag{7.10}$$

The $\alpha_k, \beta_k, \gamma_k$ and μ_k are called the new (Twiss) parameters and the new tunes.

It follows from the properties of the single-turn transfer matrix $T(s)$ that the bilinear forms

$$\tilde{z}\,(s)ST^n(s)z(s) \quad , \quad n = 1, 2, \dots \tag{7.11}$$

are independent of the s- variable; they are invariants. There are two independent invariants W_1, W_2 such that

$$\tilde{z}\,ST^n z = W_1 \sin(n\mu_1) + W_2 \sin(n\mu_2), \tag{7.12}$$

where

$$W_1 = -(\gamma_1 u^2 + 2\alpha_1 u u' + \beta_1 u'^2) = -\epsilon_1 < 0, \tag{7.13}$$

and

$$W_2 = -(\gamma_2 v^2 + 2\alpha_2 v v' + \beta_2 v'^2) = -\epsilon_2 < 0. \tag{7.14}$$

When the tune splitting is corrected, i.e., when $\mu_1 = \mu_2 = \mu$, the invariants for different n became proportional to one another. In particular, we have the relations

$$\tilde{z}\,ST^n z = \kappa_n \tilde{z}STz, \tag{7.15}$$

where

$$\kappa_n = \sin(n\mu)(\sin\mu)^{-1}, \quad n = 1, 2, \dots \ . \tag{7.16}$$

Thus it is sufficient to study only the linear in T invariant, as all other invariants yield the same family of surfaces

$$\tilde{z}\,STz = \lambda. \tag{7.17}$$

We shall consider, in some detail, the case of λ positive as it is related to the case of RHIC, for example. Hence, we consider the invariant 4-ellipsoid, $\partial\mathcal{E}_4$, defined by the above equation.

8   THE MACHINE 4-ELLIPSOID

It is convenient to employ the normalized coordinates $\overset{\circ}{z}$, cf. Equation (2.4), and write equation (7.17) in the components

$$\tilde{z}\, STz = \overset{\tilde{\circ}}{z}\, S\, \overset{\circ}{T}\overset{\circ}{z} = \sum_{k,\ell=1}^{4} \overset{\circ}{F}_{k\ell}\overset{\circ}{z}_k\overset{\circ}{z}_\ell, \tag{8.1}$$

where the coefficients are

$$\overset{\circ}{F}_{k\ell} = (S\,\overset{\circ}{T})_{k\ell} \quad , \quad k,\ell = 1,\dots,4. \tag{8.2}$$

They can be expressed through the driving terms using Equations (2.11)–(2.20). It appears useful to consider also the symmetrized coefficients defined by the expansion

$$\overset{\tilde{\circ}}{z}\, S\, \overset{\circ}{T}\overset{\circ}{z} = F_{xx}x^2 + 2F_{xx'}xx' + 2F_{xy}xy + 2F_{xy'}xy'$$
$$+ F_{x'x'}x'^2 + 2F_{x'y}x'y + 2F_{x'y'}x'y' + F_{yy}y^2 + 2F_{yy'}yy' + F_{y'y'}y'^2 = \lambda\,. \tag{8.3}$$

We have dropped the little circles since we will work, exclusively, with the circular representation. The new coefficients are:

$$
\begin{aligned}
a. &\quad F_{xx} = \overset{\circ}{M}_{21} = \overset{\vee}{F}_{yy}, \\[4pt]
b. &\quad 2F_{xx'} = \overset{\circ}{M}_{22} - \overset{\circ}{M}_{11} = 2\,\overset{\vee}{F}_{yy'}, \\[4pt]
c. &\quad 2F_{xy} = \overset{\circ}{n}_{21} + \overset{\circ}{m}_{21} = 2\,\overset{\vee}{F}_{xy}, \\[4pt]
d. &\quad 2F_{xy'} = \overset{\circ}{n}_{22} - \overset{\circ}{m}_{11} = 2\,\overset{\vee}{F}_{yx'}, \\[4pt]
e. &\quad F_{x'x'} = -\,\overset{\circ}{M}_{12} = \overset{\vee}{F}_{y'y'}, \\[4pt]
f. &\quad 2F_{x'y} = \overset{\circ}{m}_{22} - \overset{\circ}{n}_{11} = 2\,\overset{\vee}{F}_{xy'}, \\[4pt]
g. &\quad 2F_{x'y'} = -\,\overset{\circ}{n}_{12} - \overset{\circ}{m}_{12} = 2\,\overset{\vee}{F}_{x'y'}, \\[4pt]
h. &\quad F_{yy} = \overset{\circ}{N}_{21} = \overset{\vee}{F}_{xx}, \\[4pt]
i. &\quad 2F_{yy'} = \overset{\circ}{N}_{22} - \overset{\circ}{N}_{11} = 2\,\overset{\vee}{F}_{xx'}, \\[4pt]
j. &\quad F_{y'y'} = -\,\overset{\circ}{N}_{12} = \overset{\vee}{F}_{x'x'}\,.
\end{aligned}
\tag{8.4}
$$

One notes that Equation (8.3) of the invariant 4-ellipsoid stays unchanged under the transformations

$$1° \quad z \longrightarrow -z,$$
$$2° \quad z \longrightarrow \overset{\vee}{z}, \quad F \longrightarrow \overset{\vee}{F}, \tag{8.5}$$

where

$$\overset{\vee}{z} = \begin{bmatrix} y \\ y' \\ x \\ x' \end{bmatrix}, \tag{8.6}$$

and $\overset{\vee}{F}$ is obtained from F by the replacement $x \leftrightarrow y$. The first symmetry means that the $\partial\mathcal{E}_4$-ellipsoid is centered around the origin. Any plane, passing through the origin, divides $\partial\mathcal{E}_4$ into the upper, $\partial\mathcal{E}_4^{(+)}$, and the lower, $\partial\mathcal{E}_4^{(-)}$, parts, which both project onto the same sets. This may be seen clearly on the models in two and three dimensions, in Figure 2. The second symmetry reduces the algebra involved by half, since the other half of the quantities of interest follows from the first by the $\vee$ operation.

9 THE PROJECTIONS OF THE $\partial\mathcal{E}_4$ ONTO THE (X, X'), (Y, Y'), AND (X, Y) PLANES

Projecting the $\partial\mathcal{E}_4$-ellipsoid onto, say, (x', y, y') space means finding a domain on which the coordinate x_+ of the upper branch $\partial\mathcal{E}_4^{(+)}$ (or, equivalently, the lower branch $\partial\mathcal{E}_4^{(-)}$) is defined. There are four distinct projections, since the 4-ellipsoid's equation can be solved for the $x_\pm$, $x'_\pm$ and the $y_\pm$, $y'_\pm$ coordinates. In-order to see this, let us write Equation (3.3) in the four distinct forms:

$$ax^2 + bx + c = 0,$$
$$(ax^2 + bx + c)^\vee = \overset{\vee}{a}\, y^2 + \overset{\vee}{b}\, y + \overset{\vee}{c} = 0,$$
$$px'^2 + qx' + r = 0, \tag{9.1}$$
$$(px'^2 + qx' + r)^\vee = \overset{\vee}{p}\, y'^2 + \overset{\vee}{q}\, y' + \overset{\vee}{r} = 0,$$

where the coefficients are

$$a = F_{xx},$$
$$b = 2F_{xx'}x' + 2F_{xy}y + 2F_{xy'}y', \tag{9.2}$$
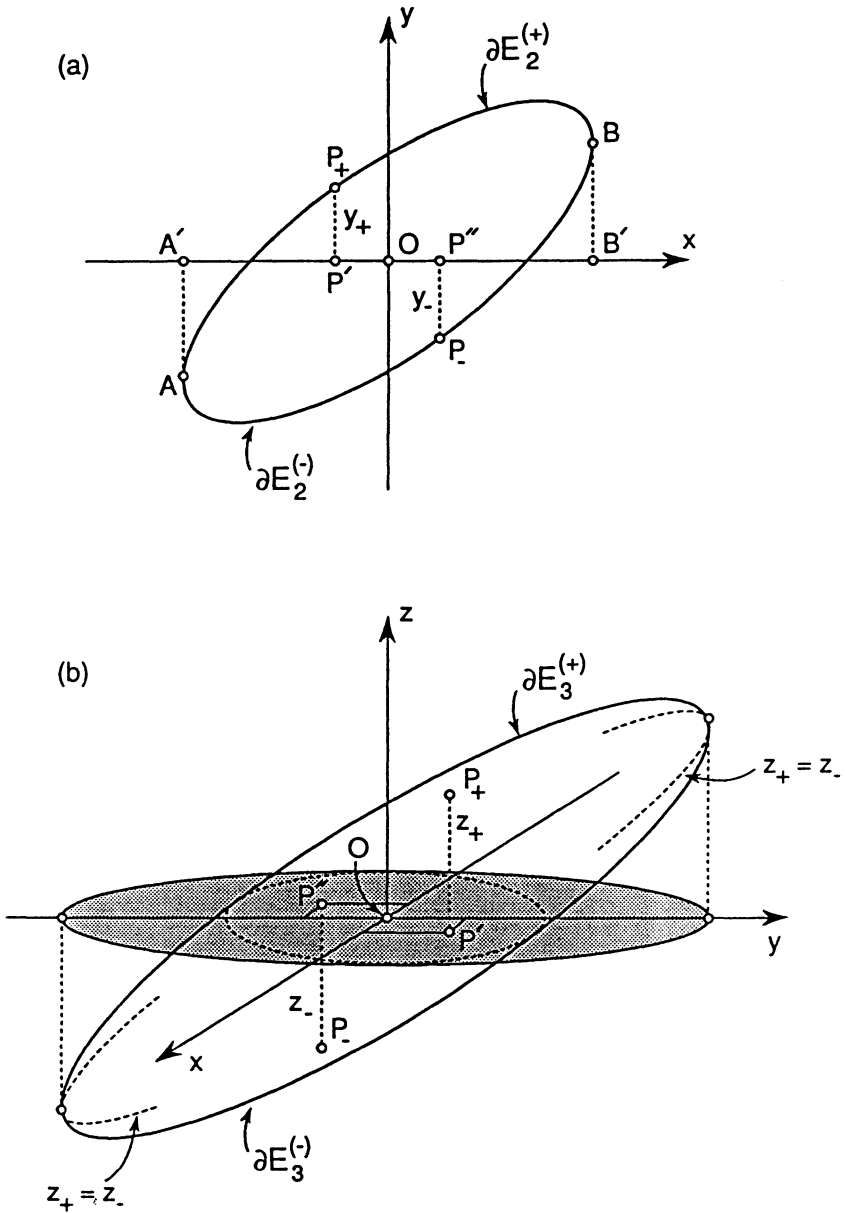$$c = F_{x'x'}x'^2 + 2F_{x'y}x'y + 2F_{x'y'}x'y' + F_{yy}y^2 + 2F_{yy'}yy' + F_{y'y'}y'^2 - \lambda,$$

FIGURE 2: Projections of the upper $y_+(z_+)$, and the lower $y_-(z_-)$ branches of the ellipse, a, and ellipsoid, b, coincide, and are symmetrically centered around the origin 6.

and

$$p = F_{x'x'},$$

$$q = 2F_{x'x}x + 2F_{x'y}y + 2F_{x'y'}y', \qquad (9.3)$$

$$r = F_{xx}x^2 + 2F_{xy}xy + 2F_{xy'}xy' + F_{yy}y^2 + 2F_{yy'}yy' + F_{y'y'}y'^2 - \lambda.$$

Hence we find for the upper and the lower branches,

$$x_\pm = \tfrac{1}{2a}(-b \pm \sqrt{b^2 - 4ac}) = x_\pm(x', y, y'),$$

$$y_\pm = (x_\pm)^\vee = y_\pm(y', x, x'),$$

$$x'_\pm = \tfrac{1}{2p}(-q \pm \sqrt{q^2 - 4pr}) = x'_\pm(x, y, y'), \qquad (9.4)$$

$$y'_\pm = (x'_\pm)^\vee = y'_\pm(x, x', y).$$

It is understood that the solutions are real, which means that the following inequalities hold:

$$b^2 - 4ac \geq 0,$$

$$\overset{\vee}{b}{}^2 - 4\,\overset{\vee}{a}\overset{\vee}{c} \geq 0,$$

$$q^2 - 4pr \geq 0, \qquad (9.5)$$

$$\overset{\vee}{q}{}^2 - 4\,\overset{\vee}{p}\overset{\vee}{r} \geq 0.$$

They define the domains, four solid 3-ellipsoids, on which the solutions $x_\pm$, etc. live. Hence, we found the projections of the 4-ellipsoid, $\partial \mathcal{E}_4$, onto $\mathcal{E}_3$, $\overset{\vee}{\mathcal{E}}_3$ and M_3, $\overset{\vee}{M}_3$, which are 3-ellipsoids, as shown in Figure 3. The surfaces, $\partial \mathcal{E}_3$ etc., of these 3-ellipsoids correspond to loci of points on the 4-ellipsoid, $\partial \mathcal{E}_4$, where the solutions x_+ and x_-, etc., coincide. They determine the boundaries of the projections, cf. Figure 2.

In the next step, we project these 3-ellipsoids onto the (x, x'), (y, y') and (x, y) planes. That is, we use only four out of the twelve distinct possibilities to project the 3-ellipsoids onto the various coordinate planes, cf. Figure 3. In principle, to find the projections one could repeat the above construction; however, another way of projecting seems more appropriate in these already imaginable cases. In-order to project, for example, the surface $\partial \mathcal{E}_3(x', y, y')$ onto the (y, y') plane, we slice it first with the planes

$$x' = c, \qquad (9.6)$$

where the parameter c varies as indicated in Figure 4, and project the intersecting ellipses onto the (y, y') plane. Taking the envelope of the projected ellipses $\partial \mathcal{E}_2(c, y, y')$ with the respect to the parameter c, one gets the ellipse $\partial \mathcal{E}_2(y, y')$. The final solid ellipse $\mathcal{E}_2(y, y')$ is now called the projection of the $\partial \mathcal{E}_4$ ellipsoid onto the (y, y') plane. To find the envelopes, one has to eliminate the parameters x', y' from the supplementary conditions.
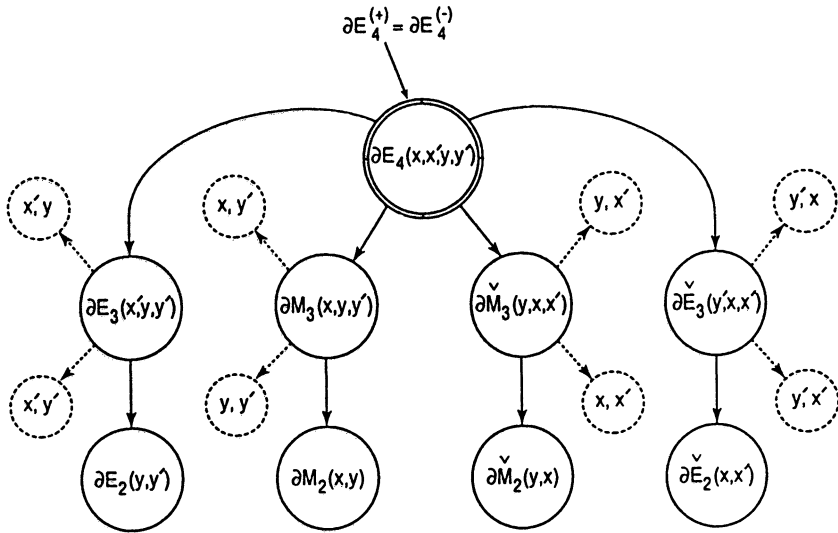
FIGURE 3: Projections of the $\partial \mathcal{E}_4$ onto the three-dimensional ellipsoids, and the ellipses of interest, as indicated by the arrows. Eight unused possibilities are indicated by the broken arrows and circles.
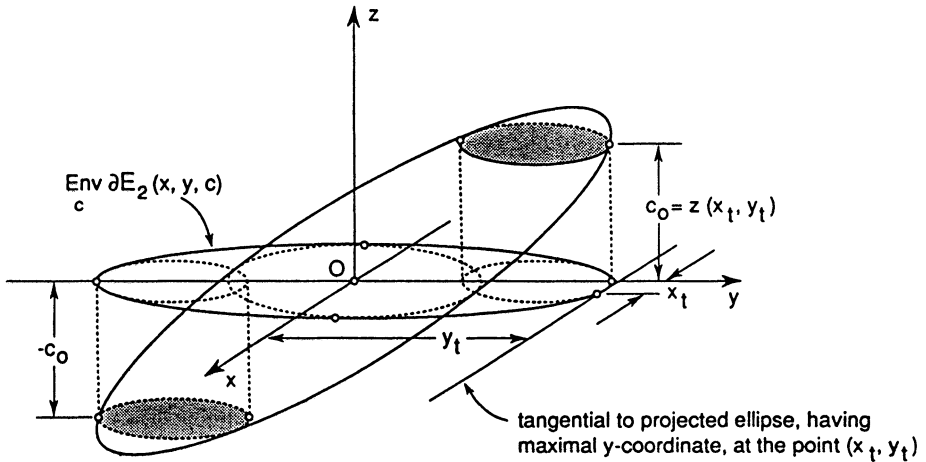

FIGURE 4: Slicing of the 3-ellipsoid with the planes $z=c, -c_0 \leq c \leq c_0$ and projecting the intersecting ellipses onto the (x,y) plane. The projected ellipses possess the elliptics' envelope.

$$\frac{\partial}{\partial x'}(b^2 - 4ac) = 0,$$

$$\frac{\partial}{\partial y'}(\overset{\vee 2}{b} - 4\overset{\vee\vee}{ac}) = 0,$$

$$\frac{\partial}{\partial y'}(q^2 - 4pr) = 0,$$ (9.7)

$$\frac{\partial}{\partial x'}(\overset{\vee 2}{q} - 4\overset{\vee\vee}{pr}) = 0.$$

Substituting the solutions back into the conditions of Equation (4.5), with the equality signs, we get the equations of the ellipses $\partial\mathcal{E}_2(y,y')$, $\partial\overset{\vee}{\mathcal{E}}_2(x,x')$ and $\partial M_2(x,y)$, $\partial\overset{\vee}{M}_2(y,x)$,:

$$\partial\mathcal{E}_2 : \quad \mathcal{E}_{yy}y^2 + 2\mathcal{E}_{yy'}yy' + \mathcal{E}_{y'y'}y'^2 = \lambda,$$

$$\partial\overset{\vee}{\mathcal{E}}_2: \quad \overset{\vee}{\mathcal{E}}_{yy}x^2 + 2\overset{\vee}{\mathcal{E}}_{yy'}xx' + \overset{\vee}{\mathcal{E}}_{y'y'}x'^2 = \lambda,$$

$$\partial M_2 : \quad M_{xx}x^2 + 2M_{xy}xy + M_{yy}y^2 = \lambda,$$ (9.8)

$$\partial\overset{\vee}{M}_2: \quad \overset{\vee}{M}_{xx}y^2 + 2\overset{\vee}{M}_{xy}yx + \overset{\vee}{M}_{yy}x^2 = \lambda,$$

where the coefficients are given in terms of the initial coefficients F up to second-order in the q's:

$$\mathcal{E}_{yy} = F_{yy} + (\sin\mu_x)^{-1}(F_{xy}^2 + F_{x'y}^2) + \cdots,$$

$$\mathcal{E}_{yy'} = F_{yy'} + (\sin\mu_x)^{-1}(F_{xy}F_{xy'} + F_{x'y'}F_{x'y}) + \cdots,$$

$$\mathcal{E}_{y'y'} = F_{y'y'} + (\sin\mu_x)^{-1}(F_{xy'}^2 + F_{x'y'}^2) + \cdots,$$

$$M_{xx} = F_{xx} + (\sin\mu_y)^{-1}F_{xy'}^2 + \cdots = \overset{\vee}{M}_{yy},$$ (9.9)

$$M_{xy} = F_{xy} + \cdots = \overset{\vee}{M}_{xy},$$

$$M_{yy} = F_{yy} + (\sin\mu_x)^{-1}F_{x'y}^2 + \cdots = \overset{\vee}{M}_{xx}.$$

Another, perhaps shorter method of projecting is described in Reference 16.

10 POSSIBLE MEASURES OF THE THICK ELLIPSE EFFECT

Let us denote the projected emittance, in absence of the linear coupling, as

$$\epsilon_x \equiv \lambda(-\sin\mu_x)^{-1},$$

$$\epsilon_y \equiv \lambda(-\sin\mu_y)^{-1},$$ (10.1)

and let us rewrite Equations (9.8) as follows

$$
\begin{array}{ll}
a. & e_{yy}y^2 + e_{yy'}2yy' + e_{y'y'}y'^2 = \epsilon_y, \\[4pt]
b. & \overset{\vee}{e}_{yy}\,x^2 + \overset{\vee}{e}_{yy'}\,2xx' + \overset{\vee}{e}_{y'y'}\,x'^2 = \epsilon_x, \\[4pt]
c. & m_{xx}x^2\epsilon_x^{-1} + m_{xy}2xy(\epsilon_x\epsilon_y)^{-1/2} + m_{yy}y^2\epsilon_y^{-1} = 1, \\[4pt]
d. & \overset{\vee}{m}_{xx}\,y^2\epsilon_y^{-1} + \overset{\vee}{m}_{xy}\,2xy(\epsilon_x\epsilon_y)^{-1/2} + \overset{\vee}{m}_{yy}\,x^2\epsilon_x^{-1} = 1,
\end{array}
\tag{10.2}
$$

where the new coefficients are

$$
\begin{aligned}
e_{yy} &\equiv \mathcal{E}_{yy}(-\sin\mu_y)^{-1}, \\
e_{yy'} &\equiv \mathcal{E}_{yy'}(-\sin\mu_y)^{-1}, \\
e_{y'y'} &\equiv \mathcal{E}_{y'y'}(-\sin\mu_y)^{-1},
\end{aligned}
\tag{10.3}
$$

and

$$
\begin{aligned}
m_{xx} &\equiv M_{xx}(-\sin\mu_x)^{-1}, \\
m_{xy} &\equiv M_{xy}(\sin\mu_x\,\sin\mu_y)^{-1/2}, \\
m_{yy} &\equiv M_{yy}(-\sin\mu_y)^{-1}.
\end{aligned}
\tag{10.4}
$$

Setting the skew quadrupole strengths q equal to zero, we get from Equations (8.4) and (8.9) the results

$$
\begin{aligned}
e_{yy}\big|_0 &= 1, & e_{yy'}\big|_0 &= 0, & e_{y'y'}\big|_0 &= 1, \\
m_{xx}\big|_0 &= 1, & m_{xy}\big|_0 &= 0, & m_{yy}\big|_0 &= 1.
\end{aligned}
\tag{10.5}
$$

Hence we recover the familiar Courant-Snyder circles (in the normalized coordinates)

$$
y^2 + y'^2 = \epsilon_y,
\tag{10.6}
$$

$$
x^2 + x'^2 = \epsilon_x,
\tag{10.7}
$$

and the ellipse in the (x, y) plane (from the last two parts of Equation (10.2)),

$$
\frac{x^2}{\epsilon_x} + \frac{y^2}{\epsilon_y} = 1.
\tag{10.8}
$$

For the averages of the coefficients e and m we get the results

$$
\begin{aligned}
\langle e_{yy}\rangle &= \langle e_{y'y'}\rangle = 1 - \kappa/4, \\
\langle m_{xx}\rangle &= \langle m_{yy}\rangle = 1 - \kappa/8, \\
\langle e_{yy'}\rangle &= \langle m_{xy}\rangle = 0,
\end{aligned}
\tag{10.9}
$$

where the parameter κ is

$$\kappa = G_0^2(\sin\mu_x \, \sin\mu_y)^{-1}. \qquad (10.10)$$

For the averages of the conjugate coefficients, one has, in general the relations

$$\langle \overset{\vee}{e} \rangle = \langle e \rangle^{\vee}, \quad \langle \overset{\vee}{m} \rangle = \langle m \rangle^{\vee}. \qquad (10.11)$$

Equation (10.2) yields

$$\begin{aligned} y^2 + y'^2 &= \epsilon_y', \\ x^2 + x'^2 &= \epsilon_x', \end{aligned} \qquad (10.12)$$

where

$$\begin{aligned} \epsilon_y' &= (1 + \kappa/4)\epsilon_y, \\ \epsilon_x' &= (1 + \kappa/4)\epsilon_x. \end{aligned} \qquad (10.13)$$

Equations (10.2c) and (10.2d), after the averaging, yield the same equation

$$\frac{x^2}{\epsilon_x''} + \frac{y^2}{\epsilon_y''} = 1, \qquad (10.14)$$

where

$$\begin{aligned} \epsilon_x'' &\equiv (1 + \kappa/8)\epsilon_x, \\ \epsilon_y'' &\equiv (1 + \kappa/8)\epsilon_y. \end{aligned} \qquad (10.15)$$

It seems that the areas enclosed between the ellipses of Equations (10.2a) and (10.6) and the corresponding curves of Equations (10.2b) and (10.7) can be considered as measures of the Thick Ellipse Effect. They are available for a spread of a trajectory when linear coupling is present. The characteristic dimensions, δ of these areas are related to the coefficients e and m (in the same-order as shown in Figure 5):

a. $\delta_y = [(e_{yy})^{-1/2} - 1]\sqrt{\epsilon_y}, \quad \delta_{y'} = [(e_{y'y'})^{-1/2} - 1]\sqrt{\epsilon_y},$

b. $\delta_x = [(\overset{\vee}{e}_{yy})^{-1/2} - 1]\sqrt{\epsilon_x}, \quad \delta_{x'} = [(\overset{\vee}{e}_{y'y'})^{-1/2} - 1]\sqrt{\epsilon_x}, \qquad (10.16)$

c. $\delta_x = [(m_{xx})^{-1/2} - 1]\sqrt{\epsilon_x}, \quad \delta_y = [(m_{yy})^{-1/2} - 1]\sqrt{\epsilon_y}.$

The areas between the curves in case a. are

$$\delta A = [(e_{yy}e_{y'y'} - e_{yy'}^2)^{-1/2} - 1]\pi\epsilon_y, \qquad (10.17)$$

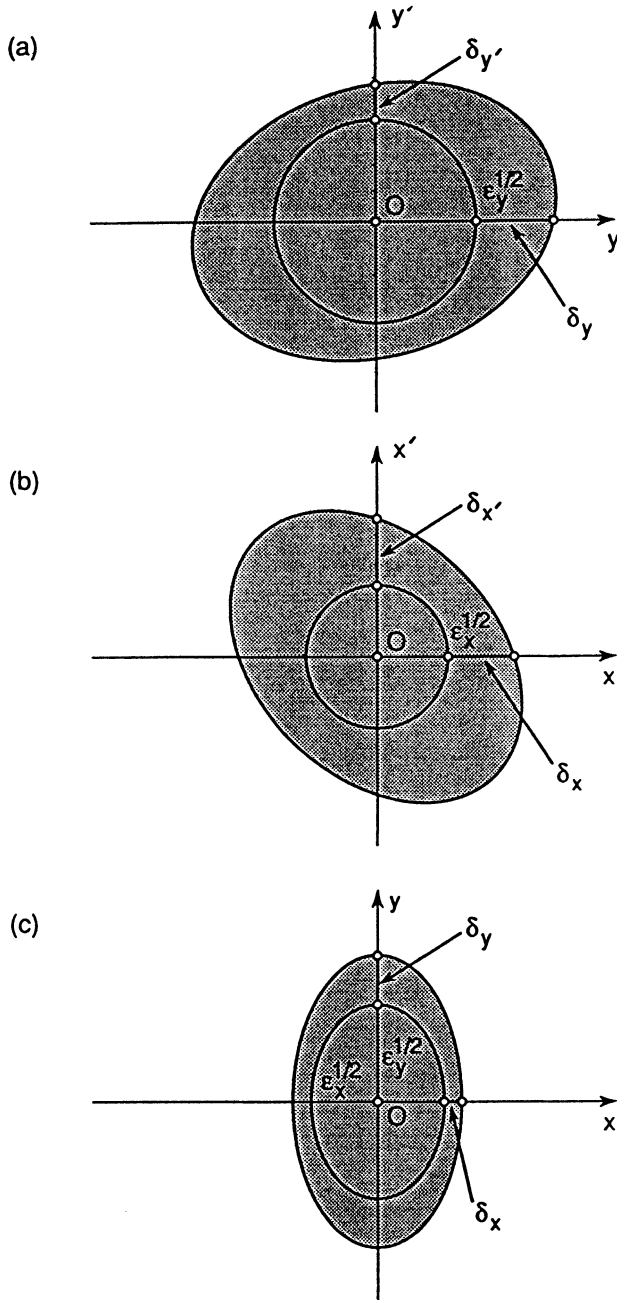and are similar for other cases.

V. GARCZYNSKI

FIGURE 5: The Thick Ellipse Effect produced by the linear coupling. The outer ellipses correspond to Equations (8.2) – (8.4), while the inner curves correspond to Equations (8.13) – (8.15).

If one performs the averaging procedure first, and then calculates the relevant characteristic dimensions, one gets the results

$$
\begin{array}{ll}
a. & \bar{\delta}_y = \bar{\delta}_{y'} = \frac{1}{8}\kappa\sqrt{\epsilon_y}, \\
b. & \bar{\delta}_x = \bar{\delta}_{x'} = \frac{1}{8}\kappa\sqrt{\epsilon_x}, \\
c. & \bar{\delta}_x = \frac{1}{16}\kappa\sqrt{\epsilon_x}, \quad \bar{\delta}_y = \frac{1}{16}\kappa\sqrt{\epsilon_y},
\end{array}
\tag{10.18}
$$

where the scale κ of the Thick Ellipse Effect is given by Equation (10.10). In the case of RHIC it is equal to

$$
\kappa_{\mathrm{RHIC}} = 0.007 . \tag{10.19}
$$

This is a rather small value to explain the observed effects as shown in Fig. 1: only a fraction of the effect can be attributed to the linear coupling alone. It seems that the bulk of it is produced by sextupoles and, possibly, by higher-multiplicity fields.

The very shape of the projected ellipses can be used for diagnosis of the linear coupling. For instance, the rotation angle ϕ_y, ϕ_x of the (y, y') and (x, x') ellipses are related to the coefficients $e_{yy'}$ etc., as follows:

$$
\tan \phi_y = -\frac{e_{yy'}}{e_{y'y'}}, \quad \tan \phi_x = -\frac{\check{e}_{yy'}}{\check{e}_{y'y'}} . \tag{10.20}
$$

They can be expressed through the driving terms using Equations (10.3), (9.9), (8.4) and (2.11)–(2.20).

The projected Equations (10.2) could be useful when matching the linearly coupled beam in a machine to another one — at the injection point, for example. The coefficients e_{yy}, $e_{yy'}$, $e_{y'y'}$ should be identified with the γ_y, α_y, β_y lattice functions of the matching beam. Similarly for the coefficients $\check{e}_{yy} = \gamma_x$, etc.

11 EMITTANCE CHANGE DUE TO LINEAR COUPLING

This problem was considered earlier by K. Brown and R. Servranckx[15] for the case of a transport line, and we follow their method supplemented, by our treatment of Δ terms, (see below). We also consider a ring case, which requires an extension of their formalism. When linear coupling is present, one considers a single 4-dimensional ellipsoid instead of two separate invariant ellipses:

$$
\tilde{z}\, \sigma^{-1} z = 1, \tag{11.1}
$$

where

$$z = \begin{bmatrix} x \\ x' \\ y \\ y' \end{bmatrix}, \tag{11.2}$$

and

$$\sigma = \begin{bmatrix} \sigma_x & \chi \\ \tilde{\chi} & \sigma_y \end{bmatrix} \tag{11.3}$$

is a symmetric and positive definite matrix while σ_x, σ_y are symmetric, positive-definite 2×2 submatrices describing projected emittance, and χ represents the linear coupling. When passing from a point s_o to another s_1 in a ring, the σ matrix transforms as follows:

$$\sigma_1 = T \sigma_0 \tilde{T} \tag{11.4}$$

when

$$z_1 = T z_0.$$

Assuming that the initial beam is decoupled ($\chi_0 = 0$), one gets the relations

$$\sigma_{x1} = M \sigma_{xo} \tilde{M} + n \sigma_{yo} \tilde{n}, \tag{11.5}$$

$$\sigma_{y1} = N \sigma_{yp} \tilde{N} + m \sigma_{xo} \tilde{m}, \tag{11.6}$$

and

$$\chi_1 = M \sigma_{xo} \tilde{m} + n \sigma_{yo} \tilde{N}. \tag{11.7}$$

The initial condition $\chi_o = 0$ is pertinent to a transport line. For a ring, a periodic boundary condition is appropriate; this requires suitable extension of the formalism as given below. Denoting the initial projected emittance as $\epsilon_{xo}, \epsilon_{yo}$, we have at the point s_o

$$\epsilon_{xo}^2 = \text{Det}\,(\sigma_{xo}), \tag{11.8}$$

and

$$\epsilon_{yo}^2 = \text{Det}\,(\sigma_{yo}), \tag{11.9}$$

and at the point s_1

$$\epsilon_{x1}^2 = \text{Det}\,(\sigma_{x1}), \tag{11.10}$$

and

$$\epsilon_{y1}^2 = \text{Det}\,(\sigma_{y1}), \tag{11.11}$$

where σ_{x1}, σ_{y1} are given by Equations (11.5) and (11.6) respectively.

Let the initial beam ellipses be upright and match perfectly the machine ellipses:

$$\sigma_{xo} = \begin{bmatrix} \sigma_{11} & \mathcal{O} \\ \mathcal{O} & \sigma_{22} \end{bmatrix} = \epsilon_{xo} \begin{bmatrix} \beta_{xo} & \mathcal{O} \\ \mathcal{O} & \beta_{xo}^{-1} \end{bmatrix}, \tag{11.12}$$

and

$$\sigma_{yo} = \begin{bmatrix} \sigma_{33} & \mathcal{O} \\ \mathcal{O} & \sigma_{44} \end{bmatrix} = \epsilon_{yo} \begin{bmatrix} \beta_{yo} & \mathcal{O} \\ \mathcal{O} & \beta_{yo}^{-1} \end{bmatrix}, \tag{11.13}$$

where we have assumed, for simplicity, that $\alpha_{xo} = \alpha_{yo} = 0$.

Using the identity

$$\text{Det}\,(A + B) = \text{Det}\,(A) + \text{Det}(B) + \begin{bmatrix} A_{11} & A_{12} \\ B_{21} & B_{22} \end{bmatrix} + \begin{bmatrix} B_{11} & B_{12} \\ A_{21} & A_{22} \end{bmatrix}, \tag{11.14}$$

one finds for the projected emittance at some point s_1 downstream,

$$\epsilon_{x1}^2 = \epsilon_{xo}^2 \text{Det}^2(M) + \epsilon_{yo}^2(n) + \Delta_x, \tag{11.15}$$

and

$$\epsilon_{y1}^2 = \epsilon_{xo}^2 \text{Det}^2(m) + \epsilon_{yo}^2(N) + \Delta_y, \tag{11.16}$$

where

$$\Delta_x = \sigma_{11}\sigma_{33} \begin{bmatrix} M_{11} & n_{11} \\ M_{21} & n_{21} \end{bmatrix}^2 + \sigma_{11}\sigma_{44} \begin{bmatrix} M_{11} & n_{12} \\ M_{21} & n_{22} \end{bmatrix}^2$$

$$+ \sigma_{22}\sigma_{33} \begin{bmatrix} M_{12} & n_{11} \\ M_{22} & n_{21} \end{bmatrix}^2 + \sigma_{22}\sigma_{44} \begin{bmatrix} M_{21} & N_{12} \\ M_{22} & n_{22} \end{bmatrix}^2, \tag{11.17}$$

and

$$\Delta_y = \sigma_{11}\sigma_{33} \begin{bmatrix} m_{11} & N_{11} \\ m_{21} & N_{21} \end{bmatrix}^2 + \sigma_{11}\sigma_{44} \begin{bmatrix} m_{11} & N_{12} \\ m_{21} & N_{22} \end{bmatrix}^2$$

$$+ \sigma_{22}\sigma_{33} \begin{bmatrix} m_{12} & N_{11} \\ m_{22} & N_{21} \end{bmatrix}^2 + \sigma_{22}\sigma_{44} \begin{bmatrix} m_{21} & N_{12} \\ m_{22} & N_{22} \end{bmatrix}^2. \tag{11.18}$$

It follows from the symplecticity of the matrix T that

$$\text{Det}\,(m) = \text{Det}\,(n) \equiv \kappa, \tag{11.19}$$

$$\text{Det}\,(M) = \text{Det}\,(N) = 1 - \kappa, \tag{11.20}$$

and

$$\Delta_x = \Delta_y \equiv \Delta. \tag{11.21}$$

Thus the projected emittance at the point s_1 is

$$\epsilon_{x1}^2 = (1 - \kappa)^2 \epsilon_{xo}^2 + \kappa^2 \epsilon_{yo}^2 + \Delta, \tag{11.22}$$

and

$$\epsilon_{y1}^2 = \kappa^2 \epsilon_{xo}^2 + (1 - \kappa)^2 \epsilon_{yo}^2 + \Delta, \tag{11.23}$$

where[8]

$$
\Delta = \epsilon_{xo}\epsilon_{yo} \left\{ \beta_{xo}\beta_{yo} \begin{bmatrix} M_{11} & n_{11} \\ M_{21} & n_{21} \end{bmatrix}^2 + \beta_{xo}\beta_{yo}^{-1} \begin{bmatrix} M_{11} & n_{12} \\ M_{21} & n_{22} \end{bmatrix}^2 \right.
$$

$$
\left. + \beta_{xo}^{-1}\beta_{yo} \begin{bmatrix} M_{12} & n_{11} \\ M_{22} & n_{21} \end{bmatrix}^2 + \beta_{xo}^{-1}\beta_{yo}^{-1} \begin{bmatrix} M_{12} & n_{12} \\ M_{22} & n_{22} \end{bmatrix}^2 \right\} \geq 0. \tag{11.24}
$$

As a result we obtain the relation[15]

$$\epsilon_{x1}^2 - \epsilon_{y1}^2 = (1 - 2\kappa)(\epsilon_{xo}^2 - \epsilon_{yo}^2). \tag{11.25}$$

Brown and Servranckx[15] consider simple consequences of this relation for a transport line, and we refer the reader to their paper for details. Instead we would like to expand their formalism to include a ring case.

Inside a circular accelerator, the proper condition in constraining the beam ellipsoid matrix is the periodic condition. In other words, Equation (11.4) now becomes

$$\sigma_1 = T\,\sigma\,\tilde{T} = \sigma = \begin{bmatrix} \sigma_x & \chi \\ \tilde{\chi} & \sigma_y \end{bmatrix}, \tag{11.26}$$

where now T stands for a single transfer matrix $T(0)$, and the subscript "o" at σ was dropped since now $s_o = 0$ can be any point in a ring, (which we also choose as a reference point in our calculations). As a result, σ is determined, and thus it is no longer possible to assume that the submatrix χ vanishes, as it was for the transfer line case.

Solving the above equation (see Appendix C for details), one finds in particular the expressions

$$\sigma_x = g^2(\rho_x + R_B \rho_y \ \tilde{R}_B),$$ (11.27)

$$\sigma_y = g^2(\rho_y + R_A \rho_x \ \tilde{R}_A),$$ (11.28)

and for the submatrix χ, which describes the coupling, one gets the result

$$\chi = g^2(\rho_x \ \tilde{R}_A + R_B \rho_y).$$ (11.29)

Here we use the notations:

$$\rho_x = \epsilon_A \begin{bmatrix} \beta_A & -\alpha_A \\ -\alpha_A & \gamma_A \end{bmatrix},$$ (11.30)

is a symmetric and positive definite matrix, and similar for ρ_y, with A replaced by B, and

$$R_A = (t + \delta)^{-1}(m + \overline{n}) = -\overline{R}_B,$$ (11.31)

and

$$g^2 = \frac{t + \delta}{2\delta},$$ (11.32)

with all the quantities being calculated at the reference point $s = 0$.

Notice that σ_x and σ_y agree with those given previously, cf. Equations (11.12) and (11.14), when the coupling is absent. This is so because $g^2 = 1$, and $R_{A,B} = 0$, and the new Twiss parameters coincide with those of the ideal lattice when the coupling vanishes. The same is true for the parameters $\epsilon_{A,B}$, which coincide with the projected emittance $\epsilon_{x,y}$. The χ submatrix vanishes, obviously, when the coupling is absent.

Equations (11.27) and (11.28) enable us to calculate the projected emittance, at the point $s = 0$, using Equations (11.8) and (11.9) and the identity (11.14):

$$\epsilon_x^2 = g^4 \left(\epsilon_A^2 + |R_B|^2 \epsilon_B^2 + \Delta_x' \right),$$ (11.33)

and

$$\epsilon_y^2 = g^4 \left(\epsilon_B^2 + |R_A|^2 \epsilon_A^2 + \Delta_y' \right),$$ (11.34)

where

$$\Delta_x' = \Delta_y' = \Delta'.$$ (11.35)

In the Thin Lens Model we find,

$$\Delta' \approx \frac{1}{4\pi^2 (\Delta\nu)^2} \left[\sum_{k,l=1}^{N} q_k q_l \cos(\mu_x^k - \mu_x^l) \cos(\mu_y^k - \mu_y^l) + \frac{1}{2}\kappa \right] 2\epsilon_A \epsilon_B , \qquad (11.36)$$

where

$$\Delta\nu = \nu_x - \nu_y. \qquad (11.37)$$

Also, using Equations (2.16–2.19) we find,

$$\kappa \approx \sum_{1 \le k < l \le N} q_k q_l \sin(\mu_x^k - \mu_x^l) \sin(\mu_y^k - \mu_y^l). \qquad (11.38)$$

Denoting

$$\zeta = \frac{t - \delta}{2\delta}, \qquad (11.39)$$

we get from Equations (B.6), (11.31), and (11.32) the results

$$g^4 |R_A|^2 = \zeta^2 \qquad (11.40)$$

and

$$g^4 = (1 - \zeta)^2 . \qquad (11.41)$$

Thus, we finally obtain the projected emittance at some point $s = 0$ in a ring:

$$\epsilon_x^2 = (1 - \zeta)^2 \epsilon_A^2 + \zeta^2 \epsilon_B^2 + \Delta' \qquad (11.42)$$

and

$$\epsilon_y^2 = (1 - \zeta)^2 \epsilon_B^2 + \zeta^2 \epsilon_A^2 + \Delta'. \qquad (11.43)$$

Subtracting both equations, one gets a relation analogous to that for a transfer line, cf. Equation (11.25), only now ζ is the relevant parameter instead of κ:

$$\epsilon_x^2 - \epsilon_y^2 = (1 - 2\zeta)(\epsilon_A^2 - \epsilon_B^2). \qquad (11.44)$$

Therefore, one may repeat the analysis and consider different cases of interest,

Case 1. If the new emittances are equal,

$$\epsilon_A = \epsilon_B , \qquad (11.45)$$

then, at any point in the ring the projected emittances coincide:

$$\epsilon_x = \epsilon_y . \qquad (11.46)$$

Case 2. If at $s = 0$

$$\zeta = \frac{1}{2} ,$$ (11.47)

then, at this point

$$\epsilon_x = \epsilon_y = \left[\frac{1}{4}(\epsilon_A^2 + \epsilon_B^2) + \Delta' \right]^{\frac{1}{2}} .$$ (11.48)

Case 3. If

$$\epsilon_A \neq 0 \quad \text{but} \quad \epsilon_B = 0 ,$$ (11.49)

then

$$\Delta' = 0 ,$$

and

$$\epsilon_x = |1 - \zeta|\epsilon_A ,$$

and (11.50)

$$\epsilon_y = |\zeta|\epsilon_A .$$

If

$$0 \leq \zeta \leq 1 ,$$ (11.51)

then

$$\epsilon_x = (1 - \zeta)\epsilon_A , \quad \epsilon_y = \zeta\epsilon_A ,$$

and, as the result, the sum becomes constant:

$$\epsilon_x + \epsilon_y = \epsilon_A .$$ (11.52)

However, if at $s = 0$

$$\zeta < 0 ,$$ (11.53)

then

$$\epsilon_x = (1 - \zeta)\epsilon_A , \quad \epsilon_y = -\zeta\epsilon_A ,$$

and the difference becomes constant:

$$\epsilon_x - \epsilon_y = \epsilon_A .$$ (11.54)

Hence the projected emittance can become large.

Similarly, if at the point $s = 0$

$$\zeta > 1 \, , \tag{11.55}$$

then

$$\epsilon_x = -(1 - \zeta)\epsilon_A \, , \quad \epsilon_y = \zeta\epsilon_A \, , \tag{11.56}$$

and again the projected emittance can be large:

$$\epsilon_y - \epsilon_x = \epsilon_A \, . \tag{11.57}$$

Similar situation arises when $\epsilon_A = 0$ but $\epsilon_B \neq 0$.

The sum of projected emittances can only exceed the sum of new emittances — in general, in accordance with inequalities analogous to Equation (58) in Ref. 15.

We can also perform relevant calculations of the projected emittance at some other point s_1 in a ring with the known emittance found for position s_o. See Reference 19 for some details.

ACKNOWLEDGMENTS

REFERENCES

1. E.D. Courant and H.S. Snyder, Ann. Phys. **3**, 1 (1958).
2. D.A. Edwards and L.C. Teng, IEEE Trans. Nucl. Sci., NS-20(3), 885 (1973).
3. L.C. Teng, *Springer Lecture Notes in Physics*, 343(4), (1989).
4. R. Talman, *Springer Lecture Notes in Physics*, 343(133), (1989).
5. L. Schachinger, T. Sun, and R. Talman, *Manual for the TEAPOT Program*, SSC Central Design Group (1990).
6. Y. Kobayashi, Nucl. Instrum. Meth. **83**, 77 (1970).
7. S. Peggs, Part. Accel., **12**, 219 (1982).
8. H. Zyngier, IEEE Trans. Nucl. Sci. NS-32(5), 2282 (1985).
9. G. Parzen, BNL Report AD/RHIC-102 (July 1991).
10. A.G. Ruggiero, in *Proceedings of the 5th ICFA Advanced Beam Dynamics Workshop* (Corpus Christi, Texas, 1991). See also BNL AD/AP Technical Note No. 29 (1991), and *Talks at Accelerator Physics Division Meetings* (1991).
11. V. Garczynski, "Beta-function distortions due to linear coupling", BNL AD/AP Technical Note No. 24 (1991).
12. V. Garczynski, "The tune shift due to linear coupling," BNL AD/AP Technical Note No. 25 (1991).
13. V. Garczynski, "Emittance change due to linear coupling: possible correction scheme of emittance growth," BNL AD/AP Technical Note No. 28 (1991).

14.   V. Garczynski, "The Thick Ellipse Effect due to linear coupling, and projections of the invariant 4-ellipsoid onto the (x,x'), (y,y') and the (x,y)-planes" BNL AD/AP Technical Note No. 33 (1991).

15.   K.L. Brown and R.V. Servranckx, "Cross-plane coupling and its effects on projected emittance," SLAC-PUB-4679 (1989).

16.   K.L. Brown, Adv. Part. Phys. (1967) 71 **1**.

17.   K.L. Brown, D.C. Carey, Ch. Iselin and F. Rothacker, SLAC 91 (1973 Rev.), NAL 91 and CERN 80–04.

18.   V. Garczynski, Nucl. Instrum. Meth. A **324** 7–13 (1993).

19.   V. Garczynski and W.T. Weng, "The tune splitting and the emittance change caused by random twists of quadrupoles and random vertical displacements of sextupoles in the AGS Booster," Booster Technical Note No. 223, BNL AGS, (1993).

APPENDIX A   Extension of the TLM to Higher Orders

The single-turn transfer matrix, in the circular representation, is given by the product

$$\overset{\circ}{T}(C,0) = \overset{\circ}{T}_0(C, s_N)\, \overset{\circ}{T}_{SQ}(s_N)\, \overset{\circ}{T}_0(s_N, s_{N-1}) \cdots \overset{\circ}{T}_0(s_2, s_1)\, \overset{\circ}{T}_{SQ}(s_1)\, \overset{\circ}{T}_0(s_1, 0), \tag{A.1}$$

where $\overset{\circ}{T}_{SQ}(s_k)$ represents the transfer matrix of the kth skew-quadrupole

$$\overset{\circ}{T}_{SQ}(s_k) = \left.\begin{bmatrix} \mathbf{1} & t \\ \hline t & \mathbf{1} \end{bmatrix}\right|_{s_k}, \tag{A.2}$$

and the 2×2 matrix t is

$$t\Big|_{s_k} = q_k(s_k) \begin{bmatrix} 0 & 0 \\ \hline 1 & 0 \end{bmatrix}, \tag{A.3}$$

where

$$q(s_k) = f_k^{-1}(\beta_x \beta_y)^{1/2}\Big|_{s_k}. \tag{A.4}$$

Equation (A.1) can be rewritten in a rather remarkable way, as it can be verified by induction, for example,[4,5]

$$\overset{\circ}{T} = \overset{\circ}{T}_N\, (\overset{\circ}{T}_0)^{-1}\, \overset{\circ}{T}_{N-1}\, (\overset{\circ}{T}_0)^{-1} \cdots \overset{\circ}{T}_2\, (\overset{\circ}{T}_0)^{-1}\, \overset{\circ}{T}_1, \tag{A.5}$$

where

$$\overset{\circ}{T}_k \equiv \overset{\circ}{T}_0(C, s_k)\, \overset{\circ}{T}_{SQ}(s_k)\, \overset{\circ}{T}_0(s_k, 0) \equiv \overset{\circ}{T}_0\, P_k, \tag{A.6}$$

where we have denoted

$$P_k \equiv \overset{\circ}{T}_0(0, s_k)\, \overset{\circ}{T}_{SQ}(s_k)\, \overset{\circ}{T}_0(s_k, 0) = \begin{bmatrix} \mathbf{1}_2 & F_k \\ \hline G_k & \mathbf{1}_2 \end{bmatrix}, \tag{A.7}$$

and

$$F_k \equiv R^{-1}(\mu_x^k) t \Big|_{s_k} R(\mu_y^k), \tag{A.8}$$

and

$$G_k \equiv R^{-1}(\mu_y^k) t \Big|_{s_k} R(\mu_x^k) = (F_k)^\vee = -\overline{F}_k, \tag{A.9}$$

where $\overline{F}$ means a symplectic conjugate of F, cf. Equation A.33.

The 4×4 matrices P_k are symplectic under these conditions. Taking into account that the inverse matrices $(\overset{\circ}{T}_0)^{-1}$ cancel inside of the product in Equation (A.5), we get finally the main formula

$$\overset{\circ}{T} = \overset{\circ}{T}_0 \; P_N \cdots P_1 = \tag{A.10}$$

$$= \left[\begin{array}{c|c} R(\mu_x) & \mathbf{0} \\ \hline \mathbf{0} & R(\mu_y) \end{array} \right] \left[\begin{array}{c|c} \mathbf{1}_2 & F_N \\ \hline G_N & \mathbf{1}_2 \end{array} \right] \cdots \left[\begin{array}{c|c} \mathbf{1}_2 & F_1 \\ \hline G_1 & \mathbf{1}_2 \end{array} \right] \equiv$$

$$\equiv \left[\begin{array}{c|c} \overset{\circ}{M} & \overset{\circ}{n} \\ \hline \overset{\circ}{m} & \overset{\circ}{N} \end{array} \right]. \tag{A.11}$$

Performing the matrix multiplication we obtain for the 2×2 submatrices

$$\overset{\circ}{M} = R(\mu_x) \left(\mathbf{1}_2 + \sum_{1 \le s_1 < s_2 \le N} F_{s_2} G_{s_1} + \cdots \right), \tag{A.12}$$

$$\overset{\circ}{N} = R(\mu_y) \left(\mathbf{1}_2 + \sum_{1 \le s_1 < s_2 \le N} G_{s_2} F_{s_1} + \cdots \right) = (\overset{\circ}{M})^\vee, \tag{A.13}$$

$$\overset{\circ}{n} = R(\mu_x) \left(\sum_{s_1=1}^{N} F_{s_1} + \cdots \right), \tag{A.14}$$

$$\overset{\circ}{m} = R(\mu_y) \left(\sum_{s_1=1}^{N} G_{s_1} + \cdots \right) = (\overset{\circ}{n})^\vee. \tag{A.15}$$

The higher-order terms are easy to find. They are products of even or odd numbers of the F's and G's intertwined. For instance, the next terms in the expansions of $\overset{\circ}{M}$ and $\overset{\circ}{n}$ matrices are, respectively,

$$\sum_{1 \le s_1 < s_2 < s_3 < s_4 \le N} F_{s_4} G_{s_3} F_{s_2} G_{S_1},$$ (A.16)

and

$$\sum_{1 \le s_1 < s_2 < s_3 \le N} F_{s_3} G_{s_2} F_{s_1}.$$ (A.17)

Since F_j, G_k are linear in q, the expansions, Equations (A.12)–(A.15) are, in fact, Nth-order polynomials in the skew-quadrupole strengths.

Further manipulations with products of 2×2 matrices, and with their sums, are facilitated by the fact that for any 2×2 real matrix A the following decomposition is valid,[6]

$$A = \begin{bmatrix} a & b \\ c & d \end{bmatrix} = A_+ + A_- \mathbf{J},$$ (A.18)

where the matrices $A_\pm$ are proportional to rotations

$$A_+ = \frac{1}{2} \begin{bmatrix} a+d & -(c-b) \\ c-b & a+d \end{bmatrix} = \sqrt{\lambda_+} R(\varphi_+),$$ (A.19)

and

$$A_- = \frac{1}{2} \begin{bmatrix} a-d & -(c+b) \\ c+b & a-d \end{bmatrix} = \sqrt{\lambda_-} R(\varphi_-),$$ (A.20)

and the matrix J is of the form

$$\mathbf{J} = \begin{bmatrix} 1 & 0 \\ 0 & -1 \end{bmatrix}.$$ (A.21)

The matrices $A_\pm$ have positive determinants

$$|A_\pm| = \frac{1}{4}[(a \pm d)^2 + (c \mp b)^2] = \lambda_\pm \ge 0,$$ (A.22)

and

$$|A| = |A_+| - |A_-| = ad - bc = \lambda_+ - \lambda_-,$$ (A.23)

and

$$Tr A = Tr A_+ = a + d = 2\sqrt{\lambda_+} \cos \varphi_+,$$ (A.24)

$$Tr(\mathbf{AJ}) = Tr A_- = a - d = 2\sqrt{\lambda_-} \cos \varphi_-.$$ (A.25)

Applying the decomposition to the t-matrix for the F_k and G_k building blocks, we obtain,

$$F_k = q_k/2R(-\pi/2)\left[R(-\mu_x^k + \mu_y^k) + R(-\mu_x^k - \mu_y^k)\mathbf{J}\right], \tag{A.26}$$

and

$$G_k = q_k/2R(-\pi/2)\left[R(\mu_x^k - \mu_y^k) + R(-\mu_x^k - \mu_y^k)\mathbf{J}\right] = \overset{\vee}{F}_k, \quad k = 1,\ldots,N \tag{A.27}$$

Hence, all the products involve only the rotation matrices R and the J matrix. They can be readily performed since the properties relate in this way:

$$R(\varphi_1)R(\varphi_2) = R(\varphi_1 + \varphi_2),$$

$$\mathbf{J}R(\varphi) = R(-\varphi)\mathbf{J},$$

$$\mathbf{J}^2 = \mathbf{1}_4. \tag{A.28}$$

In this way one can easily construct the products of F's and G's and obtain the submatrices $\overset{\circ}{M}, \overset{\circ}{n}$ to any-order in q. In particular, we can derive in this way the results

$$\overset{\circ}{M} = R(\mu_x)$$

$$+ \sum_{1 \le r < s \le N} 1/4q_r q_s \left\{ [R(\mu_x + \mu_x^r + \mu_y^r - \mu_x^s - \mu_y^s) - R(\mu_x + \mu_x^r - \mu_y^r - \mu_x^s + \mu_y^s)] \right.$$

$$\left. + [R(\mu_x - \mu_x^r + \mu_y^r - \mu_x^s - \mu_y^s) - R(\mu_x - \mu_x^r - \mu_y^r - \mu_x^s + \mu_y^s)]\mathbf{J} \right\} + \cdots, \tag{A.29}$$

and

$$\overset{\circ}{n} = \sum_{r=1}^{N} 1/2q_r [R(\mu_x - \mu_x^r + \mu_y^r - \frac{\pi}{2}) + R(\mu_x - \mu_x^r - \mu_y^r - \frac{\pi}{2})\mathbf{J}] + \cdots. \tag{A.30}$$

Using Equations (A.13) and (A.15), one gets $\overset{\circ}{N}$ and $\overset{\circ}{m}$ matrices by replacing x and y indices inside of $\overset{\circ}{M}$ and $\overset{\circ}{n}$, respectively. Thus the results shown in Equations (2.11)–(2.20) follow. One can also obtain the T matrix by applying the $\mathcal{B}^{-1}$ and $\mathcal{B}$ matrices [cf. (2.10)]

$$T = \mathcal{B}^{-1} \overset{\circ}{T} \mathcal{B}. \tag{A.31}$$

A complex notation suggests itself here, since one can associate with the components of $A_\pm$ of matrix A the complex numbers

$$A_\pm = \sqrt{\lambda_\pm} R(\varphi_\pm) \leftrightarrow \sqrt{\lambda_\pm} e^{-i\varphi_\pm}, \tag{A.32}$$

while the J-matrix becomes equivalent to a complex conjugation. The relevant calculations can thus be performed on the isomorphic complex numbers, before returning to the matrix notation.[8]

APPENDIX B   The Universal Parameterization of the Single-Turn Transfer Matrix

It was shown by Edwards and Teng,[2] and by Talman,[3] that the single-turn transfer matrix T can be brought to a quasidiagonal form as follows. If

$$T = \begin{bmatrix} M & n \\ m & N \end{bmatrix}, \tag{B.1}$$

is 4×4 real, C-periodic and symplectic, single-turn transfer matrix, then

$$U = R^{-1}TR = \begin{bmatrix} A & 0 \\ 0 & B \end{bmatrix}, \tag{B.2}$$

where A, B and R are symplectic and

$$R = g \begin{bmatrix} \mathbf{1} & \Sigma \\ -\overline{\Sigma} & \mathbf{1} \end{bmatrix}, \tag{B.3}$$

and

$$\Sigma = -\frac{1}{t + \delta}(\overline{m} + n), \tag{B.4}$$

and

$$t = \frac{1}{2}Tr(M - N), \tag{B.5}$$

$$\delta = (t^2 + |\overline{m} + n|)^{1/2} = \frac{1}{2}Tr(A - B), \tag{B.6}$$

and

$$g^2 = \frac{1}{2}\left(1 + \frac{t}{\delta}\right). \tag{B.7}$$

This parameterization of the matrix R is universal in the sense that it holds at any point of a ring. The 2×2 symplectic submatrices A and B can be parameterized in the usual way:

$$A = M + (t + \delta)^{-1}(\overline{m} + n)m \tag{B.8}$$

$$= \begin{bmatrix} \cos\mu_1 + \alpha_1\sin\mu_1 & \beta_1\sin\mu_1 \\ -\gamma_1\sin\mu_1 & \cos\mu_1 - \alpha_1\sin\mu_1 \end{bmatrix}, \tag{B.9}$$

and similarly

$$B = N - (t + \delta)^{-1}(m + \overline{n})n \tag{B.10}$$

$$= \begin{bmatrix} \dfrac{\cos\mu_2 + \alpha_2 \sin\mu_2}{-\gamma_2 \sin\mu_2} & \begin{array}{c} \beta_2 \sin\mu_2 \\ \hline \cos\mu_2 - \alpha_2 \sin\mu_2 \end{array} \end{bmatrix} \quad\text{(B.11)}$$

where $\alpha_k, \beta_k, \gamma_k = \beta_k^{-1}(1 + \alpha_k^2)$ and μ_k are called the "new" Courant-Snyder parameters and "new" tunes, respectively.

Using Equations (2.11)–(2.20) it is straightforward to derive the expansions

$$t = \frac{1}{2} Tr(M - N) = (|n| - 2)\sin[\pi(\nu_x + \nu_y)]\sin[\pi(\nu_x - \nu_y)]$$

$$+ \frac{1}{2}(d_{CC}^{(2)} + d_{SS}^{(2)} + \overset{\vee^{(2)}}{d_{CC}} + \overset{\vee^{(2)}}{d_{SS}})\cos[\pi(\nu_x + \nu_y)]\sin[\pi(\nu_x - \nu_y)] \quad\text{(B.12)}$$

$$+ \frac{1}{2}(d_{CC}^{(2)} + d_{SS}^{(2)} - \overset{\vee^{(2)}}{d_{CC}} - \overset{\vee^{(2)}}{d_{SS}})\sin[\pi(\nu_x + \nu_y)]\cos[\pi(\nu_x - \nu_y)] + 0(q^4),$$

and

$$|\overline{m} + n| = [(d_{SC}^{(1)} + d_{CS}^{(1)})^2 + (d_{CC}^{(1)} + d_{SS}^{(1)})^2]\sin^2[\pi(\nu_x + \nu_y)]$$

$$- [(d_{SC}^{(1)} - d_{CS}^{(1)})^2 + (d_{CC}^{(1)} - d_{SS}^{(1)})^2]\sin^2[\pi(\nu_x - \nu_y)] + 0(q^4).$$

$$\text{(B.13)}$$

The corresponding expansions of the δ and g parameters can be obtained from them. It follows that, on a resonance $\mu_x = \mu_y$, the determinant $|\overline{m} + n|$ is positive, for small q's, so the betatron motion can be made stable.

APPENDIX C   Solution of the Equation for σ

Using the Edwards-Teng decomposition, Equation (B.2), one may transform the equation for σ,

$$\sigma = T \, \sigma \, \widetilde{T}, \tag{C.1}$$

into the equation for $\rho = R^{-1}\sigma \, \widetilde{R}^{-1}$ as follows:

$$\rho = U \, \rho \, \widetilde{U} = \begin{bmatrix} \rho_x & \eta \\ \widetilde{\eta} & \rho_y \end{bmatrix}, \tag{C.2}$$

where

$$U = \begin{bmatrix} A & 0 \\ 0 & B \end{bmatrix}, \tag{C.3}$$

and

$$R = g \begin{bmatrix} 1 & R_B \\ R_A & 1 \end{bmatrix}, \tag{C.4}$$

with $R_{A,B}$ given by Equation (11.49), and g by Equation (11.50), while A and B are given by Equations (B.8) and (B.10), respectively. Equation (C.2) is equivalent to the following set of equations for submatrices of ρ:

$$\rho_x = A \, \rho_x \, \widetilde{A}, \tag{C.5}$$

$$\rho_y = B \, \rho_y \, \widetilde{B}, \tag{C.6}$$

and

$$\eta = A \, \eta \, \widetilde{B} \, . \tag{C.7}$$

Passing to the circular representation, we get

$$A = B_A^{-1} R(\mu_A) B_A, \tag{C.8}$$

$$B = B_B^{-1} R(\mu_B) B_B, \tag{C.9}$$

where $B_{A,B}$ and $B_{A,B}^{-1}$ are given by the new Twiss parameters, cf. Equation (2.5), and $R(\mu_{A,B})$ are rotations.

Equations (C.5) and (C.6) yield for the matrices

$$\omega_x = B_A \, \rho_x \, B_A^{-1}, \tag{C.10}$$

and

$$\omega_y = B_B \, \rho_y \, B_B^{-1}, \tag{C.11}$$

the conditions

$$\omega_x = R(\mu_A)\omega_x \, \widetilde{R}\,(\mu_A) \tag{C.12}$$

and

$$\omega_y = R(\mu_B)\omega_y \, \widetilde{R}\,(\mu_B). \tag{C.13}$$

It follows now that both matrices ω_x, ω_y are proportional to the unit, since the angles $\mu_{A,B}$ are arbitrary. Hence the results

$$\omega_x = \epsilon_A \cdot \mathbf{1}, \quad \omega_y = \epsilon_B \cdot \mathbf{1}, \tag{C.14}$$

where ϵ_A, ϵ_B are some non-negative numbers since ρ_x and ρ_y are positive-definite matrices. As a result, we get from Equations (C.10) and (C.11) the formula

$$\rho_x = \begin{bmatrix} \beta_A & -\alpha_A \\ -\alpha_A & \gamma_A \end{bmatrix} \epsilon_A, \tag{C.15}$$

and similarly for ρ_y, with $A \leftrightarrow B$.

The analysis of the Equation (C.7) yields only trivial solutions for η since the relevant determinant does not vanish; in general

$$\eta = 0. \tag{C.16}$$

Having ρ, one finds σ and Equations (11.45)–(11.47).